

See discussions, stats, and author profiles for this publication at: <https://www.researchgate.net/publication/230171556>

Application of Langmuir Probe in Recombination Dominated Afterglow Plasma

ARTICLE in BEITRÄGE AUS DER PLASMAPHYSIK · JUNE 2008

Impact Factor: 0.84 · DOI: 10.1002/ctpp.200810084

CITATIONS

17

READS

24

6 AUTHORS, INCLUDING:



I. Korolov

Magyar Tudományos Akadémia Wigner Fizi...

52 PUBLICATIONS 332 CITATIONS

SEE PROFILE



Tomas Kotrik

Bosch GmbH

37 PUBLICATIONS 265 CITATIONS

SEE PROFILE



Michal Hejduk

University of Freiburg

23 PUBLICATIONS 106 CITATIONS

SEE PROFILE



Juraj Glosik

Charles University in Prague

110 PUBLICATIONS 1,049 CITATIONS

SEE PROFILE

Application of Langmuir Probe in Recombination Dominated Afterglow Plasma

I. Korolov, T. Kotrík, R. Plašil, J. Varju, M. Hejduk, and J. Glosík*

Department of Surface and Plasma Science, Faculty of Mathematics and Physics, Charles University in Prague, V Holešovičkách 2, 180 00, Prague, Czech Republic

Received 15 October 2007, accepted 13 November 2007

Published online 13 June 2008

Key words Plasma, flowing afterglow, electron-ion recombination, FALP, KrD^+ .

PACS 34.80.Lx, 52.72.+v

New advanced data analysis method for calculation of recombination rate coefficients from the decay of electron density during the afterglow (along the flow tube) in a Flowing Afterglow Langmuir Probe (FALP) experiment is presented. The method is advantageous for measurements of recombination rate coefficients of slowly recombining ions in conditions where formation of the studied ions is slow, decaying plasma contains several types of ions and the ion formation and recombination proceed simultaneously. The new method is demonstrated on the analysis of the data obtained from plasma decay in He/Kr/H_2 and He/Kr/D_2 gas mixtures. In a limit for $[\text{Kr}]/[\text{D}_2] \gg 1$, the recombination rate coefficients for KrD^+ ions $\alpha(\text{KrD}^+, 250 \text{ K}) = 1 \times 10^8 \text{ cm}^3 \text{ s}^{-1}$ was obtained.

© 2008 WILEY-VCH Verlag GmbH & Co. KGaA, Weinheim

1 Introduction

Electron ion recombination, diffusion and ion–molecule reactions are key ion loss processes in low temperature plasma. In an experimental study of these processes, one usually creates such conditions that losses due to the process under study are dominant or can be clearly distinguished from other loss processes. For fast recombination processes with rate coefficient larger than $10^{-7} \text{ cm}^3 \text{ s}^{-1}$, Flowing Afterglow (with Langmuir Probe – FALP) is the suitable technique [1, 2] with direct determination of thermal recombination rate coefficients. For slow recombination with rate coefficients below $10^{-7} \text{ cm}^3 \text{ s}^{-1}$, FALP can be used but only with certain restrictions [3]. In this paper we discuss the FALP study of recombination processes with rate coefficients as low as $10^{-8} \text{ cm}^3 \text{ s}^{-1}$. For such slow recombination rates, diffusion losses and losses due to ion-molecule reactions have to be considered in data analysis as well. For some ions, e.g. D_3^+ , KrH^+ , KrD^+ , XeD^+ , which are formed in the afterglow in a sequence of ion molecule reactions, the formation process has to be included in the data analysis as well because recombination is not the dominant process any more. For these studies, a new method of probe data analysis was developed. To improve analysis, kinetic models have to be used for data interpretation and Electron Energy Distribution Functions (EEDF), plasma potential and electron temperature together with electron number densities have to be determined. Details of the new advanced data analysis are presented and discussed. The application of the new data analysis is demonstrated on measured data obtained during recombination studies of D_3^+ , KrH^+ and KrD^+ ions.

2 Experiment

The flowing afterglow technique was developed by Ferguson [4] over forty years ago. It is a very powerful tool for ion kinetics studies. This technique employs the principle of a chemical reactor with flowing buffer gas and reactants. The buffer – carrier gas flows through the discharge and the created plasma is carried along the flow tube, the decay of the plasma is given by the flow rate of the buffer gas. Pure helium is used as a buffer gas in majority of experiments. Reactant gases can be injected into decaying plasma by entry ports downstream from

*Corresponding author: e-mail: juraj.glosik@mff.cuni.cz

the discharge and thus the plasma composition can be changed. For plasma diagnostics, an axially movable Langmuir probe and downstream mass spectrometer are used [5, 6]. The probe is used to measure the electron density concentration at different positions along the flow tube, i.e. at different times of the plasma decay. The relation between position and decay time is given by the buffer gas velocity. The velocity on the axis of the flow tube can be determined by modulation technique. The Langmuir probe technique is well known and widely used and will not be discussed here in details [5, 7].

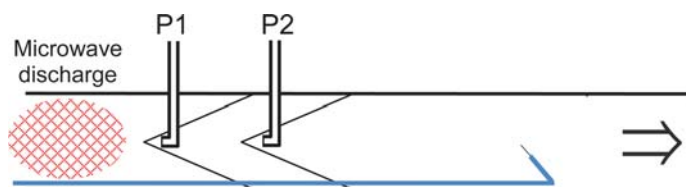


Fig. 1 The basic principle of the Flowing Afterglow with Langmuir Probe – FALP technique. Buffer gas flows from the discharge region towards the Roots pump (right side). The Langmuir probe is on the axis and it is movable from the position of the port P_2 up to the end of the flow tube.

The schema of FALP used in the presented experiments is shown in Fig. 1. Our flow tube is a stainless-steel tube with 5 cm in diameter and length over 70 cm. The carrier gas, helium at pressures 1300 – 1700 Pa and temperature near 250 K, flows through the upstream glass section of the flow tube and plasma is generated by a microwave discharge (10 – 30 W of microwave power). The flowing helium then carries the plasma into the stainless-steel section of the flow tube, where reactants are introduced via injection ports (P_1 , P_2). In the time scale: the port P_1 is ~ 3 ms downstream from the discharge region and port P_2 is another 35 ms downstream. Because the discharge is ignited in pure He, formed plasma contains electrons, He^+ ions and helium metastables. Long lived metastable atoms $\text{He}(2^3\text{S})$ and $\text{He}(2^1\text{S})$ are present in early afterglow. We will use a simple He^m symbol for both of them. Atomic He^+ ions react immediately with He atoms and in the three-body association reaction molecular He_2^+ ions are formed. The measurements are performed at high pressure of the buffer gas and at low temperatures to enhance He_2^+ formation and to prolong plasma decay. The typical electron density at position of port P_1 is $n_e \sim 5 \times 10^{10} \text{ cm}^{-3}$. Density of helium metastables is higher by at least a factor of 10, i.e. $[\text{He}^m] \sim 5 \times 10^{11} \text{ cm}^{-3}$ [8]. Krypton can be added via port P_1 to remove the helium metastables from the decaying plasma by Penning ionisation.

3 Ion formation

The method is based on the creation of well-characterised plasma that contains only desired ion species. We will discuss ion formation for a particular case, the formation of KrH^+ dominated plasma. The formation of ion KrD^+ that is also used in present study, is nearly identical and will not be discussed separately. When Kr is added via port P_1 as mentioned before, Kr^+ dominated plasma is formed in reaction of Kr with He_2^+ and He^m . After removing metastables from the plasma, electrons relax in collisions with buffer gas and a Maxwellian electron energy distribution is established [8]. The decay of the plasma can be calculated by solving a set of balance equations that include ion molecule reactions, Penning ionisation, ambipolar diffusion and recombination processes. The solution is straightforward, because electrons are thermalised (with average energy ~ 0.03 eV) and excited species with high internal energy are not present. An example of results from the numerical model of chemical kinetics in the flow tube is given in Fig. 2.

The list of processes included in the model and the corresponding rate coefficients are given e.g. in reference [9]. Lower panel of Fig. 2 shows fraction corresponding to the partial density of KrH^+ ions, $f = [\text{KrH}^+]/n_e$. Note that in the interval between 0 and 15 ms there are several ions present in the decaying plasma and KrH^+ is not the dominant ionic species. For $t > 15$ ms, KrH^+ and H_3^+ are in equilibrium, which is given by the partial pressures of Kr and H_2 . Nevertheless, the KrH^+ ion is dominant, $f \sim 0.99$, and the decay of plasma is governed by its recombination. The numerical model helps to find the right experimental conditions for which the ion or ions to be studied are dominant in the reaction zone. The results are also used in data analysis.

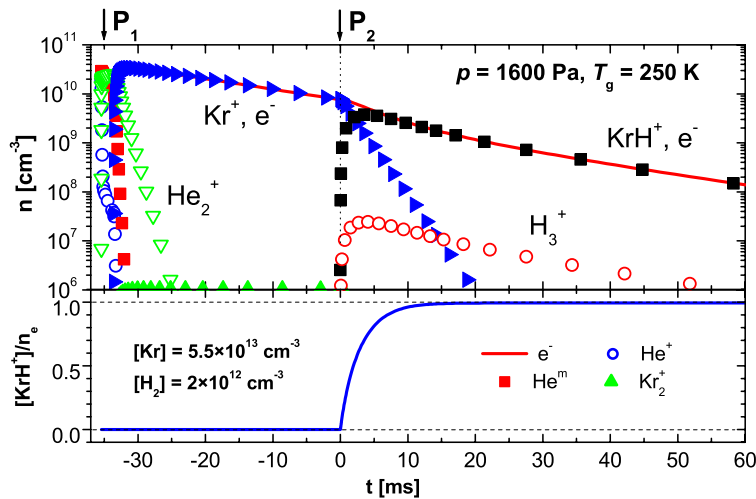


Fig. 2 The plasma decay in Flowing Afterglow calculated with the kinetic model. Kr is added via port P₁ and H₂ is added via port P₂. For the used reactant concentrations the formation of desired ions is slow. In lower panel, ratio of the formed KrH⁺ to the electron concentrations is plotted, $\xi(t) = [\text{KrH}^+]/n_e$. (Online colour: www.cpp-journal.org).

4 Plasma decay and data analysis

Numerical modelling of KrH⁺ formation presented in the previous section has shown that the transformation of Kr⁺ to KrH⁺ can proceed along a considerable part of the flow tube, especially with a very low concentration of reactants Kr and H₂ (see Fig. 3).

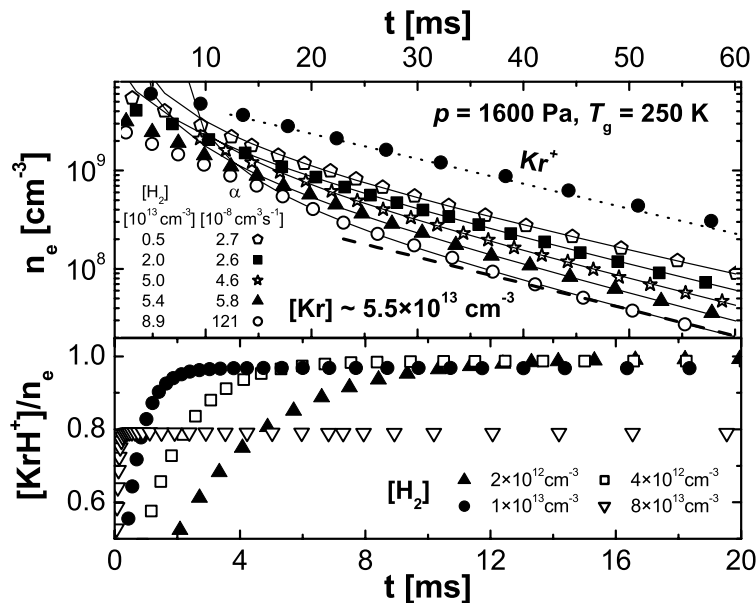


Fig. 3 **Upper panel:** A selection of electron density decays measured in a He/Kr/H₂ mixture at $T = 250$ K for several concentrations of H₂ and constant Kr density. The indicated fits consider only recombination and diffusion; see discussion below. **Lower panel:** The calculated fraction of KrH⁺ in the decaying plasma for [H₂] changing from 10¹² cm⁻³ to 10¹⁴ cm⁻³. Note the different time scales in upper and lower panel.

In that case there is a risk that the common methods of rate coefficient determination from the slope of a graph of the reciprocal of the electron density $n_e(t)$ versus decay time will be not accurate enough. For this reason, an advanced data analysis procedure has been developed. Low reactant densities are used to avoid formation of fast recombining cluster ions, which would substantially enhance the overall recombination process.

When recombination is the dominant loss process in the afterglow, the balance equation for electron concentration n_e in quasineutral plasma and the analytical solution for recombination of one dominant ion are:

$$\frac{dn_e}{dt} = -\alpha n_+ n_e = -\alpha n_e^2; \quad \frac{1}{n_e(t)} = \frac{1}{n_e(t=0)} + \alpha t, \quad (1)$$

where $n_e \equiv [e^-] = \sum [A_i^+]$ and A_i^+ represents all ion types in the flow tube. The commonly used method for determining recombination rate coefficient is based on fitting the plot of $1/n_e(t)$ versus t with a linear function, α is obtained as the slope.

When plasma decays due to reaction with species B and diffusion losses are not negligible with respect to recombination losses, the balance equation has to be extended to

$$\frac{dn_e}{dt} = -\alpha n_e^2 - k n_e [B] - \frac{D_a}{\Lambda^2} n_e = -\alpha n_e^2 - n_e/\tau; \quad \text{where } 1/\tau = k[B] - \frac{D_a}{\Lambda^2}, \quad (2)$$

where k is the reaction rate coefficient, D_a ambipolar diffusion coefficient, Λ is given by the geometry of the flow tube and τ is characteristic time of reaction and diffusion losses [10, 11]. In this case, the following analytical solution exists:

$$\frac{1}{n_e(t)} = \frac{1}{n_e(t=0)} e^{t/\tau} + \alpha (e^{t/\tau} - 1) \tau \quad (3)$$

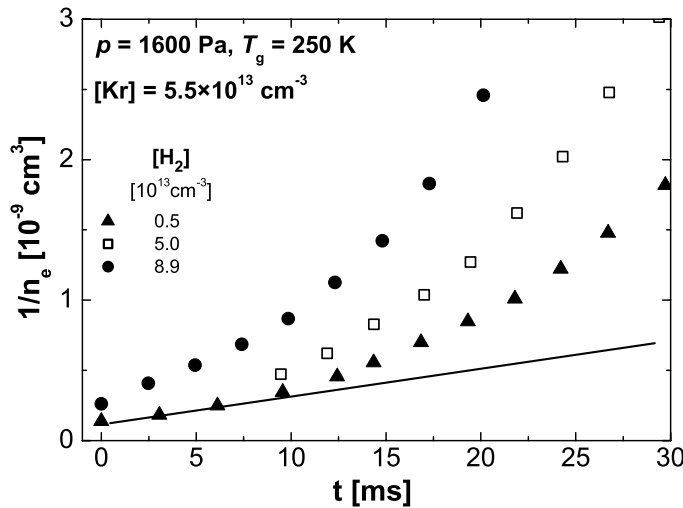


Fig. 4 Reciprocal of the electron density $n_e(t)$ versus decay time for constant Kr and several H_2 densities. The data come from the Kr sets used in Fig. 3.

Fig. 4 shows a sub-set of data sets from those in Fig. 3 plotted as $1/n_e$ versus decay time t . This projection is often used for the determination of recombination rate coefficient using formula (1). It is obvious that the plot is far from being linear and such a simple analysis cannot be applied in this case. The formula (3) is used to fit the data in the upper panel in Fig. 3. Note that at low decay time the fits are very problematic. It is not surprising, because in the discussed case the ion under study (KrH^+) is not dominant during first 15 ms of the decay after port P_2 . Nevertheless, we can use the fact that Kr^+ recombine very slowly, so the losses due to Kr^+ recombination can be neglected in comparison with recombination of KrH^+ ions. In this sense, we can write the balance equation:

$$\frac{dn_e}{dt} = -\alpha \xi(t) n_e^2 - n_e/\tau, \quad \text{where } [KrH^+] = \xi(t) n_e, \quad 0 \leq \xi \leq 1. \quad (4)$$

Using simple integration we obtain

$$\ln \left[\frac{n_e(t_b)}{n_e(t_a)} \right] + (t_b - t_a)/\tau = -\alpha \int_{t_a}^{t_b} \xi(t) n_e(t) dt, \quad (5)$$

where t_a and t_b are integration limits and τ is expected to be a constant factor independent on time. If the desired ion is dominant in the afterglow $\xi(t) = 1$, then a plot of

$$\ln \left[\frac{n_e(t_b)}{n_e(t_a)} \right] + (t_b - t_a)/\tau \text{ versus } \int_{t_a}^{t_b} n_e(t) dt \quad (6)$$

should give straight line with slope $-\alpha$. This is assured only if the correct value of the constant τ is used; otherwise the graph is curved. The correct value of τ is determined by minimizing the χ^2 of the linear fit where τ is the varied parameter. The analysis requires further discussion when $\xi(t) < 1$. Formula (5) can be expanded to

$$\ln \left[\frac{n_e(t_b)}{n_e(t_a)} \right] + (t_b - t_a)/\tau = -\alpha \int_{t_a}^{t_b} n_e(t) dt - \alpha \int_{t_a}^{t_b} (\xi(t) - 1) n_e(t) dt. \quad (7)$$

Let t_a be a fixed parameter and $t_b > t_a$ the variable parameter scanning over all data points starting from t_a , then the second integral term on the right side increases with increasing t_b as long as $(1 - \xi(t)) > 0$. For higher t_b the studied ion becomes dominant and $\xi = 1$ and thus the integral does not increase. In another words, the second integral term does not differ for t_b scanning over the zone where the studied ion is dominant and acts only as a constant. Then the plot described by (6) is again a straight line with $-\alpha$ as slope. The y -axis term $\ln[n(t_b)/n(t_a)] + (t_b - t_a)/\tau$ can also be interpreted as the normalization of data to $n(t_a)$ and subtraction of diffusion losses. The remaining part yields extracted recombination losses. An example of data plotted using formula (6) is given in Fig. 5.

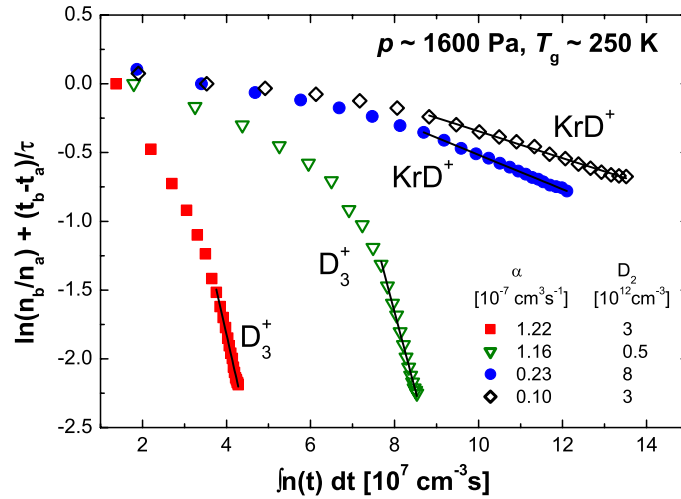


Fig. 5 Advanced analysis: Plot of $\ln[n(t_b)/n(t_a)] + (t_b - t_a)/\tau$ versus $\int n_e(t) dt$. The data were measured for two D₂ densities for KrD⁺ and D₃⁺ ions. The rate coefficients of recombination of KrD⁺ and D₃⁺ ions are noted in the figure. (Online colour: www.cpp-journal.org).

The data were obtained in study of recombination of KrD⁺ for different mixtures of D₂ and Kr. As was already mentioned, formation kinetics of KrD⁺ ions is similar to the just discussed formation of KrH⁺ ions, so it will be not repeated here. The example with KrD⁺ is given because the recombination rate coefficient for this ion is smaller than the coefficient for KrH⁺ by a factor of two.

The data in KrD⁺ study were measured for several different D₂ densities. In these measurements Kr was added via port P₁, $[\text{Kr}] = 2.3 \times 10^{13} \text{ cm}^{-3}$. The increase of the measured recombination rate coefficients with

increasing D_2 density indicates formation of faster recombining D_3^+ ions. The low D_2 density limit gives binary recombination rate coefficient, $\alpha(KrD^+, 250\text{ K}) = 1 \times 10^{-8} \text{ cm}^3 \text{ s}^{-1}$. The data in D_3^+ study were measured for two different D_2 densities. They are plotted in Fig. 5 for demonstration. In these measurements Ar was added via port P_1 , $[Ar] = 1.4 \times 10^{13} \text{ cm}^{-3}$. Obtained is effective recombination rate coefficient, $\alpha_{\text{eff}}(D_3^+, 250\text{ K}) = 1.2 \times 10^{-7} \text{ cm}^3 \text{ s}^{-1}$. We are using attribute “effective” to emphasize the fact that D_3^+ recombination in afterglow plasma is pressure dependent, similar to H_3^+ recombination, and it is not pure binary process [12].

5 Conclusion

A new advanced data analysis method for calculation of recombination rate coefficients from the decay of electron density along the flow tube in FALP experiment was developed. The advantages of this data analysis in comparison with the standard fitting of $n_e(t)$ with equation (3) are:

- Linear fitting is easier and more precise than fitting by a nonlinear equation (3) with 3 fitted parameters ($n_e(t=0)$, α , τ).
- The “ion formation zone” is visually more distinguishable, especially for very low α .
- The diffusion losses (τ) can be easily determined from decays where $n_e(t)$ decrease due to recombination is negligible with respect to diffusion (long time t , late afterglow).

The effective recombination rate coefficients in the mixture of Kr and D_2 were obtained using the here described advanced analysis method. The values of measured effective recombination rate coefficients are dependent on the relative population of D_3^+ and KrD^+ ions (on ξ), which is given by ratio $[Kr]/[D_2]$. In equation (7) ξ is constant but $\xi < 1$, the effective recombination rate can be then measured as a function of $[Kr]/[D_2]$ and the rate coefficient for KrD^+ ion can be obtained by extrapolation towards $[Kr]/[D_2] \gg 1$. In the present study, for $[Kr]/[D_2] \gg 1$ we have obtained the recombination rate coefficient, $\alpha(KrD^+, 250\text{ K}) = 1 \times 10^{-8} \text{ cm}^3 \text{ s}^{-1}$. Detailed FALP studies of several slowly recombining ions using the presented data analysis are in progress and are reported elsewhere [2, 12].

Acknowledgements This work is a part of the research plan MSM 0021620834 financed by the Ministry of Education of the Czech Republic.

References

- [1] A.I. Florescu-Mitchell and J.B.A. Mitchell, *Physics Reports* **430**, 277 (2006).
- [2] O. Novotny, R. Plasil, A. Pysanenko, I. Korolov, and J. Glosik, *J. Phys. B: At., Mol. Opt. Phys.* **39**, 2561 (2006).
- [3] J. Glosik, O. Novotny, A. Pysanenko, P. Zakouril, R. Plasil, P. Kudrna, and V. Poterya, *Plasma Sources Sci. Technol.* **12**, S117 (2003).
- [4] E.E. Ferguson, F.C. Fehsenfeld, D.B. Dunkin, A.L. Schmeltekopf, and H.I. Schiff, *Planetary and Space Science* **12**, 1169 (1964).
- [5] R. Plasil, J. Glosik, and P. Zakouril, *J. Phys. B: At. Mol. Opt. Phys.* **32**, 3575 (1999).
- [6] R. Plasil, J. Glosik, V. Poterya, P. Kudrna, J. Ruzs, M. Tichy, and A. Pysanenko, *Int. J. Mass Spectrom.* **218**, 105 (2002).
- [7] J.D. Swift and M.J.R. Schwar, *Electrical Probes for Plasma Diagnostics* (Iliffe, London, 1970).
- [8] I. Korolov, R. Plasil, T. Kotrik, P. Dohnal, O. Novotny, and J. Glosik, *Contrib. Plasma Phys.* this volume.
- [9] I. Korolov, O. Novotny, R. Plasil, P. Hlavenka, T. Kotrik, M. Tichy, P. Kudrna, J. Glosik, and A. Luca, *Czech. J. Phys.* **56**, 854 (2006).
- [10] F. Chen, *Introduction to Plasma Physics and Controlled Fusion* (Plenum Press, New York, 1984).
- [11] D. Smith and P. Spanel, *Int. J. Mass Spectrom. Ion Processes* **129**, 163 (1993).
- [12] J. Glosik, I. Korolov, R. Plasil, O. Novotny, T. Kotrik, P. Hlavenka, J. Varju, C.H. Greene, V. Kokoouline, and I.A. Mikhailov, *Phys. Rev. Lett.* sent for publication (2007).